

Article

# Analysis of Electroencephalograms Based on the Phase Plane Method

Oksana Kharchenko<sup>1</sup>, Zlatinka Kovacheva<sup>1,2</sup> and Velin Andonov<sup>1,\*</sup> 

<sup>1</sup> Institute of Mathematics and Informatics, Bulgarian Academy of Sciences, Acad. Georgi Bonchev Str., Block 8, 1113 Sofia, Bulgaria; kharchenko@math.bas.bg (O.K.); zkovacheva@math.bas.bg (Z.K.)

<sup>2</sup> Department of Mathematics and Informatics, University of Mining and Geology, Prof. Boyan Kamenov Str., 1700 Sofia, Bulgaria

\* Correspondence: velin\_andonov@math.bas.bg; Tel.: +359-877-220-981

**Abstract:** Ensuring noise immunity is one of the main tasks of radio engineering and telecommunication. The main task of signal receiving comes down to the best recovery of useful information from a signal that is destructed during propagation and received together with interference. Currently, the interference and noise control comes to the fore. Modern elements and methods of processing, related to intelligent systems, strengthen the role of the verification and recognition of targets. This makes noise control particularly relevant. The most-important quantitative indicator that characterizes the quality of the useful signal is the signal-to-noise ratio. Therefore, determining the noise parameters is very important. In the present paper, a signal model is used in the form of an additive mixture of useful signals and Gaussian noise. It is an ordinary model of a received signal in radio engineering and communications. It is shown that the phase portrait of this signal has the shape of an ellipse at the low noise level. For the first time, an expression of the width of the ellipse line is obtained, which is determined by the noise dispersion. Currently, in electroencephalography, diagnosis is based on the Fourier transform. But, many brain diseases are not detected by this method. Therefore, the search and use of other methods of signal processing is relevant.

**Keywords:** phase portrait; signal-to-noise ratio; electroencephalogram; wavelet transform



**Citation:** Kharchenko, O.; Kovacheva, Z.; Andonov, V. Analysis of Electroencephalograms Based on the Phase Plane Method. *Appl. Sci.* **2024**, *14*, 2204. <https://doi.org/10.3390/app14052204>

Academic Editors: Gang Wei, Patrik Kamencay, Roman Radil and Jakub Misek

Received: 1 December 2023

Revised: 23 February 2024

Accepted: 24 February 2024

Published: 6 March 2024



**Copyright:** © 2024 by the authors. Licensee MDPI, Basel, Switzerland. This article is an open access article distributed under the terms and conditions of the Creative Commons Attribution (CC BY) license (<https://creativecommons.org/licenses/by/4.0/>).

## 1. Introduction

The expansion of the functions and tasks of information exchange is one of the most-important trends in the modern development of society. At the same time, the role of information systems that ensure the transmission, reception, and processing of information with the required quality and in specified time intervals increases significantly. The use of a unified energy information carrier—the electromagnetic field—significantly increases the importance of radio engineering systems for receiving and processing signals operating in a wide range of frequencies, both in pulsed and continuous modes.

The complexity of the problem is significantly aggravated due to a sharp increase in the number of signal sources, which leads to an increase in the integral background of electromagnetic interference. This complicates the task of the useful signal standing out. Along with natural noise, which includes the internal noise of radio receivers, atmospheric and industrial interference, signal fluctuations, reflection from the underlying surface, etc., in the channels of radio engineering systems, several radio systems for various purposes operate simultaneously on the same or adjacent sections of the frequency range. Based on this, the search for new methods of signal processing is relevant.

Despite the high information content and compactness, the phase plane did not become a tool for analyzing processes in radio engineering and telecommunication systems. The phase plane is a less-commonly used method in signal processing than the amplitude spectrum. However, there are applications of this method to EEG, audio signals, etc. [1–4].

This work aims to expand the application of this method and to show its advantages in the visualization and determination of the SNR, also in the case of EEG.

## 2. Phase Plane Method

A phase portrait is a graphical representation of a dynamical system, which is described by a system of differential equations. It allows us to visualize the change in the state of the system as a function of time. A phase portrait is constructed in a coordinate plane, where each point represents the state of the system at a certain point in time. The coordinate axes correspond to the variables of the system's state.

The phase portrait allows us to analyze the behavior of the system, determine the stability of its states, and find points of equilibrium. It can also help in predicting the future behavior of the system and determine the optimal parameters to achieve the desired results.

To build a phase portrait, it is necessary to:

- Define the system state variables. These can be physical quantities such as position, speed, temperature, etc.;
- Define differential equations that describe how the variables of the state of the system change over time. These equations can be derived from physical laws or experimental data;
- Solve the differential equations for different initial conditions to obtain the values of the variables of the state of the system at different points in time;
- Draw points corresponding to the values of the state variables on the coordinate plane. Each point represents the state of the system at a particular point in time;
- Connect the points with lines or curves to obtain a phase portrait. The shape and nature of these lines or curves can provide information about the behavior of the system.

The phase portrait can be supplemented with additional elements such as phase trajectories, phase flows, and phase lines. These elements can help to visualize and analyze the behavior of the system in detail.

A phase portrait is a graphical representation of the states of a system as a function of time. It consists of several basic elements: equilibrium points, phase trajectories, phase lines.

The phase portrait is a powerful tool for analyzing and understanding the dynamics of a system. It is used in various fields of science and technology: mechanics and physics, biology, economics, and finance. In radio engineering, the phase portrait is used to analyze the dynamics of electrical circuits. For example, when analyzing the operation of a generator of electromagnetic oscillations, both harmonic and relaxation, the phase portrait allows us to determine different modes of operation.

The phase plane method is a qualitative method for studying both the stationary and transient regimes, including nonlinear systems. In fact, this method is reduced to the numerical solution of a second-order differential equation. The main advantage of the phase plane method is its suitability for the analysis of nonlinear systems. Some important features of nonlinear systems, which are impossible or difficult to study analytically, can be studied using graphoanalytical constructions on the phase plane [5].

The phase trajectory is a set of points; the horizontal coordinate corresponds to the system function, and the vertical coordinate is its derivative at each moment of time.

The phase portrait (PP) shows all possible system operation regimes at any initial conditions. In particular, it is possible to observe limit cycles, if they exist. Besides, the PP illustrates the stability of limit cycles, and the shape of limit cycles reflects the oscillations shape [6,7].

If the equations of a system are presented in canonical form, then the state vector of the system uniquely determines its state. Using the phase plane method, the behavior of the nonlinear system under study is considered and described, not in the time domain (that is, in the form of equations of processes in the system), but in the phase space of the system (that is, in the form of phase trajectories). Each state of the system in the state space corresponds to a point. The depicted point moves over time, describing the phase trajectory.

From this point of view, time is a parameter: the phase trajectory equation is given by the relationship between the function and its velocity.

Visually, the phase trajectory and phase portrait can be represented in the case of a two-dimensional phase space. The two-dimensional phase space is called the phase plane; this is a coordinate plane in which two variables (phase coordinates) are placed along the coordinate axes, which uniquely determines the state of the second-order system. The speed of movement is placed along the ordinate axis and displacement along the abscissa axis of the phase plane [8–10].

Based on the phase portrait, conclusions can be drawn about the nature of transient processes. The phase portrait provides the necessary information about the behavior of the system, which is described by a nonlinear equation. The phase portrait shows all possible modes for any initial conditions. In particular, boundary cycles, if they exist, are noticeable. Based on the phase portrait, conclusions can be drawn about the stability of boundary cycles. The shape of the boundary cycles expresses the shape of the oscillations. The phase plane method is widely used in the theory of nonlinear devices, as it helps to simply and clearly illustrate the nature of oscillations [11–14].

However, it is convenient to study nonlinear systems by constructing a phase portrait only in the case of a second-order system, when the phase trajectories are placed on a plane [15,16].

Let us determine the phase trajectory of the harmonic oscillation:  $x = A\cos(\omega t + \phi)$ , then  $v = x' = -A\omega\sin(\omega t + \phi)$ .

Let us exclude time by adding  $x^2$  and  $(x')^2$ . We obtain

$$\frac{x^2}{A^2} + \frac{v^2}{(A\omega)^2} = 1. \tag{1}$$

On the phase plane, Equation (1) describes an ellipse with half-axes  $A$  and  $A\omega$  (Figure 1). The ellipse turns into a circle at  $\omega = 1$ . However, a circle can be obtained for any frequency by changing the ordinate axis scale [17,18].

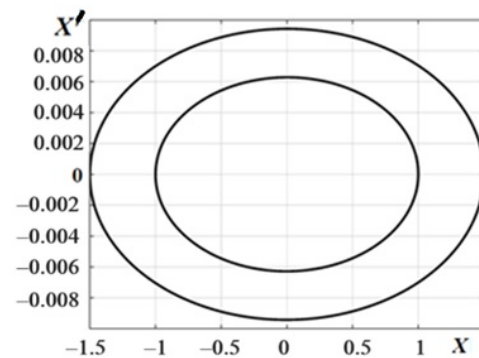


**Figure 1.** Harmonic oscillations the PP of different amplitudes.

Let us consider a different kind of signal. For the triangular signal, the velocity is piecewise constant. In this case, the phase trajectory is a rhombus (Figure 2).

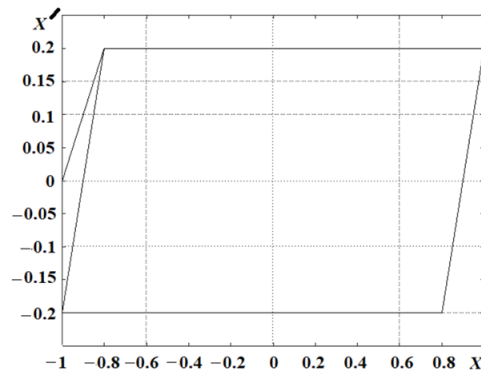


Figure 2. PP of triangular oscillation.

### 3. Determination of the Signal-to-Noise Ratio Based on the Phase Portrait

The possibilities of the phase plane method are considered in the analysis of stochastic processes. First, we consider Gaussian noise with zero mean value and standard deviation  $\sigma = 1$ . The Gaussian noise PP is shown in Figure 3.

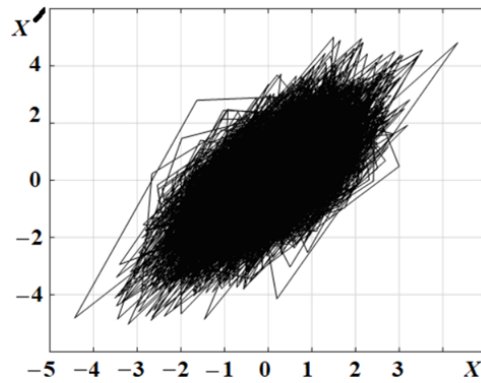


Figure 3. Gaussian noise PP.

In Figure 3, it is seen that the deviation from the mean practically does not exceed 3, i.e., the 3-sigma rule is carried out [17]. Along the ordinate axis, the derivative of the normal process has been placed. Let us define its mean value and dispersion using the statistics' basic formulas [18,19].

The obtained results are given in Table 1.

Table 1. Statistical parameters of the normal process derivative.

Probability Density Function	Mean Value	Dispersion
$\begin{cases} \frac{x}{2\sigma^2} \exp\left(-\frac{x^2}{2\sigma^2}\right), & \text{if } x \geq 0 \\ \frac{-x}{2\sigma^2} \exp\left(-\frac{x^2}{2\sigma^2}\right), & \text{if } x \leq 0 \end{cases}$	0	$2\sigma^2 = 2$

The probability density function of the normal process derivative is shown in Figure 4.

The resulting probability density function characterizes a new random process, which has zero mean value, and the values of the process are concentrated in the interval  $-4\sigma \leq x' \leq 4\sigma$ . This is shown in Table 2.

One of the most-commonly used models of a received signal in radio engineering and communications is the additive mixture of useful signals and noise. In radio engineering and communications, the Gaussian random process is a mathematical model of active and passive interferences, atmospheric and cosmic noise, fading channels, and channels with multipath propagation. The receiver's fluctuation noises also have a normal law of

distribution [19]. The adequacy of this model for many real interferences and signals and its universality are explained by the central limit theorem of the probability theory.

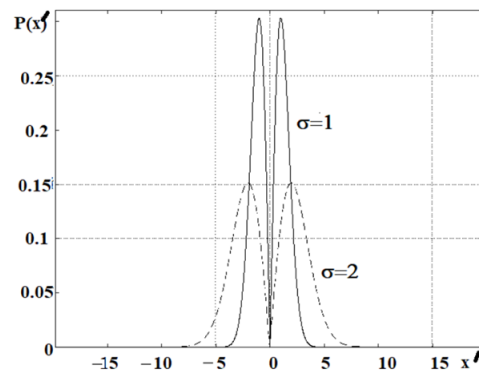


Figure 4. Probability density function of the normal process derivative.

Let us consider the signal PP at different signal-to-noise ratios (SNRs) (Figure 5). The harmonic signal is a useful signal, and Gaussian noise is an interference.

From the figures (Figure 5), it can be seen that the PP of the additive mixture of the harmonic signal and normal noise has an ellipse form and the ellipse line width is a function of the noise power.

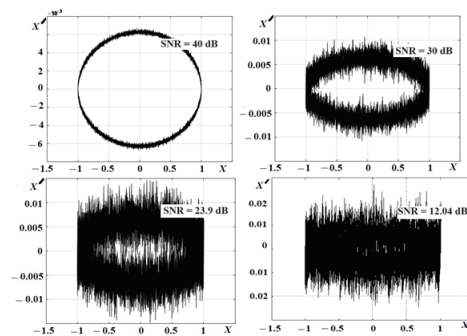


Figure 5. PP of the sum of harmonic oscillation and Gaussian noise.

Since the differentiation operation is linear, it is possible to determine the ellipse line width. To do this, the probability of  $x' = y$  should be defined in certain limits.

The probability of  $x' = y$  should be in the range  $[-a, a]$  and  $P(-a \leq y \leq a) = [1 - \exp(-y^2/2\sigma^2)]$ .

Let us determine this probability at different values of the parameter  $a$ . The results are shown in Table 2.

Table 2. Probability of  $x' = y$  at different values of the parameter  $a$ .

$a$	$2\sigma$	$3\sigma$	$4\sigma$
$P(-a \leq y \leq a)$	0.8647	0.9889	0.9997

Therefore, the ellipse line thickness is determined by the value of  $8\sigma$ . Obviously, for the phase portrait of the additive mixture of the harmonic signal and normal noise to have the form of an ellipse, the following condition should be satisfied:

$$A\omega \sin(\omega t + \phi)/4\sigma > 1. \tag{2}$$

#### 4. Electroencephalogram Phase Portrait and Wavelet Analysis

Numerical methods in biomedical research belong to a rapidly developing field, which provides a state-of-the-art tool for biomedical research and applications. These methods are

currently applied in medicine, specifically in neuroscience, cardiology, and pathology. Data processing has currently become one of the most-active fields of neuroscience, in particular in the processing of electroencephalograms (EEGs).

An EEG is a broadband oscillatory process in which, however, certain dominant harmonic constituents exist. The total EEG reflects the functional activity of the brain. Changes in the brain's functional activity are quite unambiguously reflected in the EEG.

Therefore, in modern studies, EEG indicators are among the most-important in assessing the level of functional activity in clinical neurophysiology and psychophysiology [20,21].

The spectrum of the EEG is quite complicated. The classification of EEG rhythms by some basic ranges is introduced. The concept of "rhythm" in the EEG refers to a certain frequency band matching to a certain brain condition. The main rhythms are given in Table 3 [20,21].

**Table 3.** EEG rhythms.

EEG rhythms of an awake adult		
rhythm	Frequency (Hz)	Amplitude ( $\mu\text{V}$ )
$\alpha$	8 ÷ 13	up to 100
$\beta$	14 ÷ 40	up to 15 normally 3 ÷ 7
Types of pathological activity for an awake adult		
$\delta$	0.5 ÷ 3	exceeds 40 $\mu\text{V}$ , reaching 300 $\mu\text{V}$ or more in some pathological conditions
$\theta$	4 ÷ 6	– $\ll$ –

The most-widely used method in clinical practice is the study of the signal spectrum, which is, to some extent, comparable to the manual amplitude–frequency analysis of the EEG. This method is highly informative and visual when assessing EEG components. As in manual analysis, the problem of determining the ratio of various rhythmic components in a complex EEG and determining their individual expression is solved. For this purpose, the Fourier transform (FT) is used. The FT is used when it is necessary to visually assess the holistic dynamics of the EEG during long-term observation or functional tests. In this case, the spectra for successive epochs are displayed, drawn one after the other. But, unfortunately, this method of EEG analysis does not allow diagnosing many brain diseases, for example Parkinson's and Alzheimer's diseases. Therefore, the use of other methods of EEG analysis is relevant.

The ability to accurately quantify EEG parameters allows for a more-detailed and objective assessment of dynamic changes in the functional state of the brain, which turn out to be more-informative than assessing the differences between normal and pathological conditions using manual research methods. Using the power spectrum, you can easily obtain a picture of the EEG distribution over the rhythms and determine the dominant rhythm and the dominant frequency of both the entire EEG and each individual rhythm.

The use of numerical methods in studying the rhythms of the biopotentials of the brains of patients with local lesions made it possible to obtain quantitative, objective assessments of EEG disorders. In addition, the use of numerical methods expands the diagnostic and, in cases of severe conditions, prognostic capabilities of EEG.

The fact that EEG is a broadband oscillatory process, in which, however, certain dominant harmonics can be identified, is proof that brain neurons synchronize their work

with each other. Otherwise, the sum of many thousands or even millions of electrical potentials of individual nerve cells would constitute quasi-white noise. Changes in the functional activity of the brain are reflected quite clearly in the EEG. The connection between these changes and EEG changes is so close that, in modern studies, EEG indicators are one of the most-important in assessing the level of functional activity in clinical neurophysiology and psychophysiology.

The EEG rhythms of an awake adult person include the alpha, beta, and gamma rhythms [22–25].

The alpha rhythm is characterized by a frequency in the range of  $8 \div 13$  Hz, with an amplitude up to  $100 \mu\text{V}$ . It is registered in  $85 \div 95\%$  of healthy adults examined. It is best expressed in the occipital regions; in the anterior direction, its amplitude gradually decreases. Healthy people are characterized by a relatively narrow range of the  $\alpha$  rhythm. The  $\alpha$  rhythm has the greatest amplitude in a state of calm, relaxed wakefulness. Its amplitude varies significantly over time. Spontaneous changes in amplitude, the so-called “spindles”, are observed quite regularly, expressed in alternating increases and decreases in amplitude. With an increase in the level of the functional activity of the brain (intense attention, intense mental work, etc.), the amplitude of the  $\alpha$  rhythm decreases, and often, it completely disappears. High-frequency irregular activity appears in the EEG.

The beta rhythm is characterized by a frequency in the range of  $14 \div 40$  Hz and an amplitude up to  $15 \mu\text{V}$ . The  $\beta$  rhythm is best recorded in the area of the anterior central gyri, but also extends to the posterior central and frontal gyri. Normally, it is very weakly expressed and usually has an amplitude of  $3 \div 7 \mu\text{V}$ . If there are artifacts, they can completely camouflage themselves. The  $\beta$  rhythm is associated with motor cortical mechanisms and produces an extinction reaction in response to motor activation. When moving, the  $\beta$  rhythm disappears in the zone of the corresponding cortical projection.

In Figure 6, the EEG of an healthy adult person is shown. Since the frequency band  $0.5 \div 40$  Hz is informative, the signal is filtered by a bandpass filter with cutoff frequencies of 0.4 and 45 Hz. This figure clearly shows the nonstationarity of the EEG.

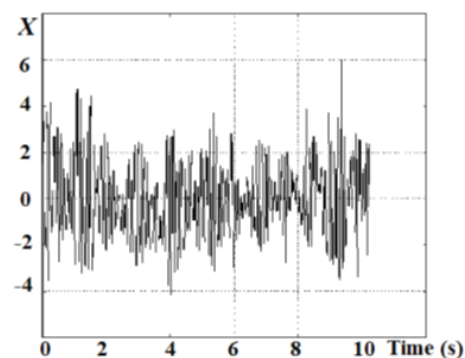


**Figure 6.** EEG of an awake adult.

The spectrum of this implementation is shown in Figure 7. It is incorrect to use the spectral method in the case of a nonstationary signal, but, nevertheless, it has found wide application in electroencephalography, because it allows obtaining an approximate idea of EEG rhythms.

In this figure, a high level of the  $\alpha$  rhythm can be observed, which is natural in a state of quiet wakefulness. Other rhythms are weakly expressed. The EEG is essentially uniform across the entire brain and symmetrical. However, the functional heterogeneity of the cortex leads to peculiarities in the electrical activity of different areas of the brain. However, due to a fairly gradual transition from one functional zone of the cortex to another, the change in EEG types along the length of the cortex occurs gradually.

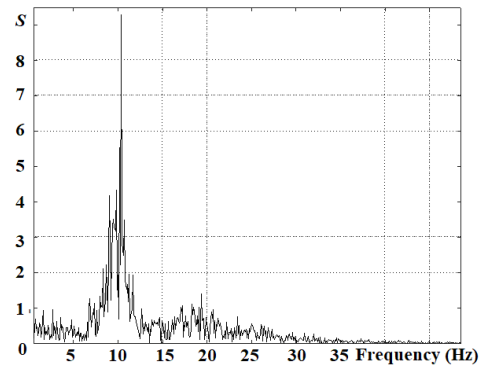


**Figure 7.** EEG amplitude spectrum of the awake adult shown in Figure 6.

One of the main criteria when analyzing the EEG is symmetry. EEG symmetry means a significant coincidence of frequencies, amplitudes, and phases of symmetrical areas of the two hemispheres of the brain. Based on the prevalence of asymmetric pathological oscillations, they predict hemispheric disorders, when the changes cover the entire hemisphere, and focal ones, which are usually expressed under one electrode.

The frequency–amplitude characteristics of the EEG described above are characteristics of a healthy, awake person.

Pathological manifestations in the EEG include the appearance of slow rhythms: theta ( $\theta$ ) and delta ( $\delta$ ). The lower their frequency and higher the amplitude, the more pronounced the pathological process is. The theta rhythm is characterized by a frequency of  $4 \div 6$  Hz, and the amplitude exceeds  $40 \mu\text{V}$ , reaching  $300 \mu\text{V}$  or more in some pathological conditions. The  $\delta$  rhythm is characterized by a frequency of  $0.5 \div 3$  Hz, and the amplitude is the same as that of the  $\theta$  rhythm. In the EEG of an awake adult person, there may also be  $\theta$  and  $\delta$  rhythms of short duration and with an amplitude not exceeding the amplitude of the  $\alpha$  rhythm. In this case, they speak of a certain decrease in the level of the functional activity of the brain.

One of the important aspects of the use of the EEG is the study of epilepsy. Data from modern research indicate that the brain in epilepsy is characterized by a number of functional rearrangements at the macro- and micro-structural level.

Let us consider the implementation of the EEG of a person with epilepsy (Figure 8). The same filtering was performed here as in the previous case (Figure 6). This implementation differs from the implementation shown in Figure 6, even visually. It can be seen that it contains slow components.

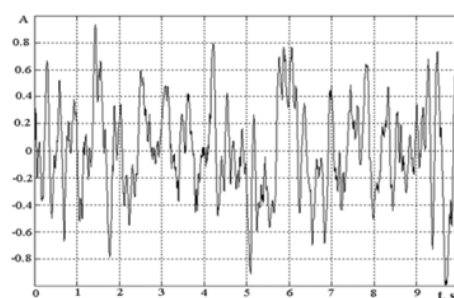


**Figure 8.** Implementation of an EEG of a person with epilepsy.

The spectrum of this implementation is shown in Figure 9. It contains powerful frequency components in the ranges of the  $\theta$  and  $\delta$  rhythms and practically does not contain the  $\alpha$  rhythm.



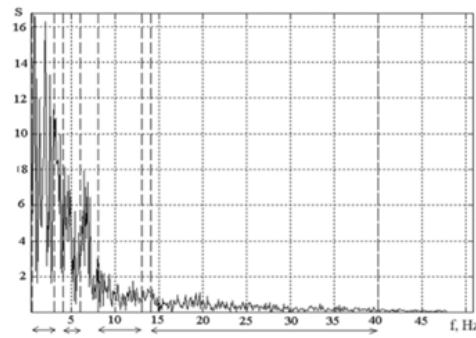


Figure 9. The spectrum of the EEG implementation shown in Figure 8.

The features of the EEG signal characterize it as nonstationary and broadband. In the case of a nonstationary process, the Fourier transform does not provide any time information. This method allows seeing the frequencies contained in the signal, but does not allow determining at what time interval of the oscillations certain frequencies exist. Therefore, the Fourier transform can be used to analyze nonstationary signals when only frequency information is of interest, and the lifetime of the spectral components is not important. In addition, a frequency component that is small in amplitude and duration may not be detected in the spectral plot.

The variety of factors influencing the statistical properties of physiological processes largely cause their nonstationarity, which leads to the need to search for adequate methods for the statistical analysis of the EEG. This determines the wide variety of methods for the statistical processing of the EEG [26–28].

The PP of this EEG implementation (Figure 10) has the form of an ellipse. This confirms the conclusion that the mathematical model of the EEG is an additive mixture of harmonic components and Gaussian noise [29]. But, in three cases, the PP of this EEG implementation does not have the form of an ellipse, due to the random character of the EEG.

The SNR can be determined based on the phase portrait. The power of the sinusoidal oscillation is  $A^2/2$  (see [1]). The noise power in this case is  $(4\delta)^2 = 16\delta^2$ . From this, we obtain  $SNR = A^2/32\delta^2$ . The results are shown in Table 4. It can be seen that, with the help of the PP, it is possible to obtain the statistical characteristics of the EEG, which can be used in diagnostics.

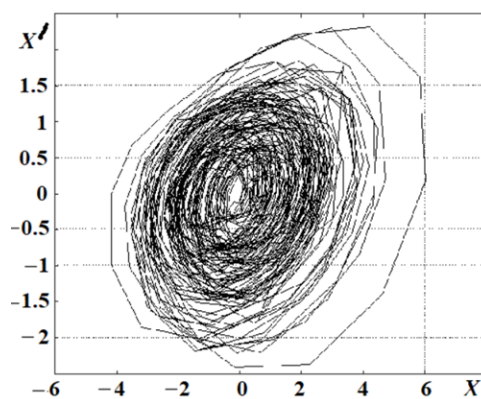


Figure 10. EEG PP of the awake adult shown in Figure 6.

Table 4. SNR of EEG.

Number of Realizations of EEG	1	2	3	4	5	6	7
SNR	22.1	23.5	23.1	22.9	23.1	22.7	23.4

Recently, the wavelet transform (WT) has been widely used in the study of biomedical signals, given their nonstationarity, and, in particular, in EEG processing [30–34]. This method makes it possible to numerically characterize the duration and change of the basic physiological rhythms, as well as to trace the change in frequency in time within each rhythm. In addition, it allows the distribution of power over the frequency ranges to be traced.

The wavelet transform decomposes the original signal into its approximation and detail components, followed by refinement by the iterative method. Each step of such a refinement corresponds to a certain level of signal decomposition and reconstruction. To realize this possibility, there are series of orthogonal wavelets. They are created based on the representation of the signal space as a system of nested subspaces, which differ from each other only by changing the scale of the independent variable [31,35].

This type of analysis is based on the following premises:

- Signal space  $v$  can be divided into nested subspaces  $v_j$  that do not intersect;
- For any function  $s(t) \in v_j$ , its compressed version belongs to the space  $v_{j-1}$ ;
- There is a function  $\phi(x) \in v_0$ , the shifts of which  $\phi_{0,k} = \phi(t - k)$  create the orthonormal basis of space  $v_0$ .

Functions  $\phi_{j,k} = 2^{-j/2} \phi(2^{-j}t - k)$  create the orthonormal basis of the space.

The reconstruction of the signal at the resolution  $n$ -level  $j_n$  is determined by the expression:

$$s(t) = \sum_{k=-\infty}^{\infty} a_{j_n,k} \phi_{j_n,k}(t) + \sum_{j=j_n}^{\infty} \sum_{k=-\infty}^{\infty} d_{j,k} \psi_k(t), \tag{3}$$

where  $a$  is the approximation coefficient;  $d$  is the detail coefficient.

Let us apply the WT to the implementation of the EEG shown in Figure 6. Simlet wavelets were used. These wavelets belong to orthogonal wavelets with a compact carrier; they are close to symmetrical ones [36].

Let us decompose the EEG implementation (Figure 6) into an approximation ( $a_5$ ) and five detail coefficients ( $d_1 \div d_5$ ) (Figure 11). This method is similar to frequency analysis using bandpass filters.

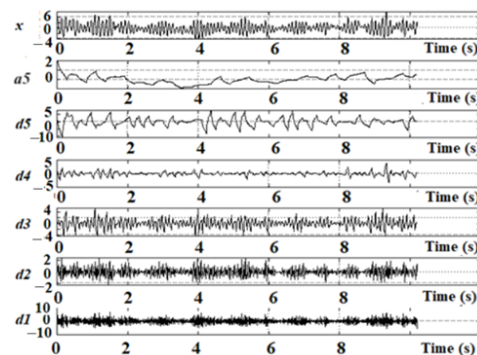
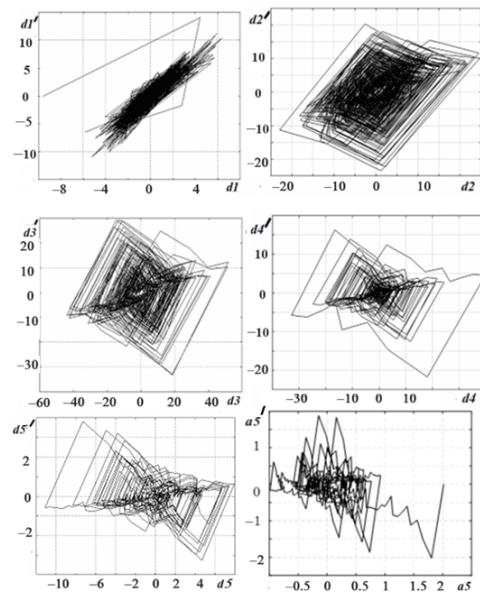


Figure 11. WT of the EEG implementation shown in Figure 6.

All detail coefficients of the PP were built (Figure 12). The PP of the coefficient  $d_1$  looks like a noise PP. The remaining coefficients have the appearance of a rhombus.

For more details, coefficients  $d_2$  and  $d_3$  are shown in Figure 13. The hole observed on the PP indicates that the oscillations are a mixture of the harmonic signal and the fairly small noise level in these frequency bands. Therefore, the power of the noise is not evenly distributed over the frequency range. This is observed for the EEGs of all ten awake adults.

Let us determine the spectrum of these detail coefficients. The amplitude spectrum of the detail component  $d_2$  is shown in Figure 14. Peaks are reached at frequencies  $f = 10; 20; 40$  Hz.



**Figure 12.** Detail coefficients of the PP of the EEG WT.

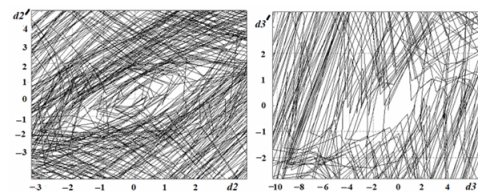


**Figure 13.** PP of the detail coefficients  $d2$  and  $d3$  (more details).

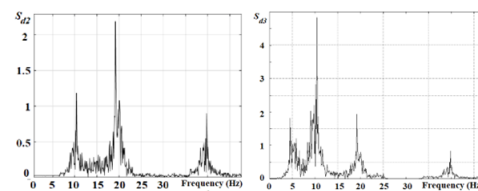


**Figure 14.** Amplitude spectrum of detail coefficients  $d2$  and  $d3$ .

The amplitude spectrum of the detail component  $d3$  is shown in Figure 14. Peaks are reached at frequencies  $f = 5; 10; 20$  Hz.

The considered amplitude spectra show that the main harmonic components are at frequencies  $f = 5; 10; 20; 40$  Hz.

## 5. Conclusions

The main task of signal reception is to recover as much useful information about the signal as possible, which is distorted during propagation and received along with interference.

The amplitude spectrum is widely used in signal processing, and the PP is undeservedly forgotten in this processing.

The most-important quantitative indicator that characterizes the quality of the useful signal is the SNR.

For the first time, using an additive mixture of the signal and noise, it can be seen that, at a sufficiently low noise level ( $SNR \geq 23.9$  in our case), the PP has the shape of an ellipse, and the ellipse line width is determined by the value of  $8\sigma$ .

The free space inside the ellipse disappears with an increase in noise power, and the PP has the form of a noise PP.

The condition when the phase portrait of the additive mixture of the harmonic signal and normal noise has the form of an ellipse has been obtained.

EEGs of ten awake adults were considered. By constructing the EEG PP of an awake adult, an ellipse was obtained. This form of the PP allows assuming that the mathematical model of the EEG is an additive mixture of harmonic components and Gaussian noise.

Currently, wavelet analysis is widely used in applied problems in the analysis of nonstationary signals. The application of the discrete WT and PP to the EEG makes it possible to determine the harmonic components. The main harmonic components are at frequencies  $f = 5; 10; 20; 40$  Hz for the EEG under consideration. The EEG noise power is shown to be not evenly distributed over the frequency range, which opens up the prospects for the use of this method in the diagnosis of diseases and studies of the functional activity of the brain. These methods can be installed in the form of the software and hardware implementations of modern encephalographs, which will increase the reliability of the analysis and ensure the reproducibility of the results.

**Author Contributions:** Conceptualization, O.K. and Z.K.; methodology, O.K.; software, O.K.; formal analysis, O.K., Z.K. and V.A.; investigation, O.K. and Z.K.; writing—original draft preparation, O.K., Z.K. and V.A.; writing—review and editing, V.A., O.K. and Z.K. All authors have read and agreed to the published version of the manuscript.

**Funding:** This work was supported by a grant from The Simons Foundation International (grant No. 992227, IMI-BAS).

**Institutional Review Board Statement:** Ethical review and approval were waived from this study because of patient anonymity.

**Informed Consent Statement:** Patient consent was waived due to the patient anonymity.

**Data Availability Statement:** The data presented in this study are available on request from the corresponding author. The data are not publicly available due to privacy restrictions.

**Conflicts of Interest:** The authors declare no conflicts of interest.

## References

1. Collura, T.F.; Morris, H.H.; Burgess, R.C.; Jacobs, E.C.; Klem, G.H. Phase-plane trajectories of EEG seizure patterns in epilepsy. *Am. J. EEG Technol.* **1992**, *32*, 295–307. [\[CrossRef\]](#)
2. Akilli, M.; Yilmaz, N. Study of weak periodic signals in the EEG signals and their relationship with postsynaptic potentials. *IEEE Trans. Neural Syst. Rehabil. Eng.* **2018**, *26*, 1918–1925. [\[CrossRef\]](#)
3. Jarray, R.; Jmail, N.; Hadriche, A.; Frikha, T. A Comparison between modeling a normal and an epileptic state using the FHN and the epileptor model. In *Innovations in Bio-Inspired Computing and Applications, Proceedings of the 8th International Conference on Innovations in Bio-Inspired Computing and Applications (IBICA 2017), Marrakech, Morocco, 11–13 December 2017*; Springer International Publishing: Berlin/Heidelberg, Germany, 2018; pp. 245–254.
4. Kako, T.; Ohishi, Y.; Kameoka, H.; Kashino, K.; Takeda, K. Automatic Identification for Singing Style based on Sung Melodic Contour Characterized in Phase Plane. In *Proceedings of the 10th International Society for Music Information Retrieval Conference, Kobe, Japan, 26–30 October 2009*; pp. 393–398.
5. Voloshchuk, Y.I. *Signals and Processes in Radiotechnics*; OO “Company Smith”: Kharkiv, Ukraine, 2005; Volume 2, pp. 102–121.
6. Vidyasagar, M. *Nonlinear Systems Analysis*; Society for Industrial and Applied Mathematics: Philadelphia, PA, USA, 2002; p. 515.
7. Reyn, J. *Phase Portraits of Planar Quadratic Systems*; Springer: Berlin/Heidelberg, Germany, 2007; pp. 35–115.
8. Kudryashov, N.A.; Lavrova, S.F. Painlevé Test, Phase Plane Analysis and Analytic Solutions of the Chavy–Waddy–Kolokolnikov Model for the Description of Bacterial Colonies. *Mathematics* **2023**, *11*, 3203. [\[CrossRef\]](#)
9. Melka, R.F.; Yousif, H.A. Imaging phase plane models. *Int. J. Math. Educ. Sci. Technol.* **2023**, *54*, 2281–2303. [\[CrossRef\]](#)
10. Tenreiro Machado, J.A.; Costa, A.C.; Quelhas, M.D. Shannon, Rényi and Tsallis entropy analysis of DNA using phase plane. *Nonlinear Anal. Real World Appl.* **2011**, *12*, 3135–3144. [\[CrossRef\]](#)
11. Tamang, J.; Abdikian, A.; Saha, A. Phase plane analysis of small amplitude electron-acoustic supernonlinear and nonlinear waves in magnetized plasmas. *Phys. Scr.* **2020**, *95*, 105604–105623. [\[CrossRef\]](#)
12. Amir, M. Phase-plane analysis of test particle orbits in regular black holes. *Commun. Theor. Phys.* **2020**, *72*, 15404–15411. [\[CrossRef\]](#)
13. Mantaras, D.; Luque, P.; Alonso, M. Phase plane analysis applied to non-explicit multibody vehicle models. *Multibody Syst. Dyn.* **2022**, *56*, 173–188. [\[CrossRef\]](#)
14. Isojima, S.; Suzuki, S. Ultradiscrete hard-spring equation and its phase plane analysis. *Jpn. J. Ind. Appl. Math.* **2023**, *40*, 1083–1105. [\[CrossRef\]](#)

15. Streipert, S.; Wolkowicz, G. An augmented phase plane approach for discrete planar maps: Introducing next-iterate operators. *Math. Biosci.* **2023**, *355*, 121–132. [[CrossRef](#)]
16. Tchernichovski, O.; Benjamini, Y.; Golani, I. The dynamics of long-term exploration in the rat. Part I. A phase-plane analysis of the relationship between location and velocity. *Biol. Cybern.* **1998**, *78*, 423–432. [[CrossRef](#)]
17. Encyclopedia of Mathematics. “Three-Sigma Rule”. Available online: [https://encyclopediaofmath.org/wiki/Three-sigma\\_rule](https://encyclopediaofmath.org/wiki/Three-sigma_rule) (accessed on 20 December 2023).
18. Middleton, D. *An Introduction to Statistical Communication Theory: An IEEE Press Classic Reissue*; Wiley-IEEE Press: Hoboken, NJ, USA, 1996; pp. 275–351.
19. Levin, B.R. *Theoretical Foundations of Statistical Radiotechnics*; Radio and Communications: Moscow, Russia, 1989; pp. 57–104.
20. Zenkov, L.R. *Pharmacoresistent Epilepsy*; Medpress-Inform: Vydavets, Russia, 2003; pp. 11–21.
21. Zenkov, L.R. *Clinical Encephalography with Elements of Epileptology*; Medpress-Inform: Vydavets, Russia, 2016; pp. 13–31.
22. Purdon, P.; Pavone, K.; Akeju, O. The Ageing Brain: Age-dependent changes in the electroencephalogram during propofol and sevoflurane general anaesthesia. *Br. J. Anaesth. BJA* **2015**, *115*, i46–i57. [[CrossRef](#)]
23. Struck, A.; Osman, G.; Rampal, N. Time-dependent risk of seizures in critically ill patients on continuous electroencephalogram. *Ann. Neurol.* **2017**, *82*, 177–185. [[CrossRef](#)]
24. Gao, Y.; Gao, B.; Chen, Q. Deep Convolutional Neural Network-Based Epileptic Electroencephalogram (EEG) Signal Classification. *Front. Neurol.* **2020**, *11*, 375. [[CrossRef](#)]
25. Friedman, D. Continuous Electroencephalogram Monitoring in the Intensive Care Unit. *Anesth. Analg.* **2009**, *109*, 506–523. [[CrossRef](#)]
26. Runnova, A.; Zhuravlev, M.; Ukolov, R.; Blokhina, I.; Dubrovski, A.; Lezhnev, N.; Sitnikova, E.; Saranceva, E.; Kiselev, A.; Karavaev, A.; et al. Modified wavelet analysis of ECoG-pattern as promising tool for detection of the blood–brain barrier leakage. *Sci. Rep.* **2021**, *11*, 18505. [[CrossRef](#)]
27. Rossetti, A.O.; Schindler, K.; Sutter, R.; Rüegg, S.; Zubler, F.; Novy, J.; Oddo, M.; Warpelin-Decrausaz, L.; Alvarez, V. Continuous vs. Routine Electroencephalogram in Critically Ill Adults with Altered Consciousness and No Recent Seizure. A Multicenter Randomized Clinical Trial. *JAMA Neurol.* **2020**, *77*, 1225–1232. [[CrossRef](#)] [[PubMed](#)]
28. Chaumon, M. A practical guide to the selection of independent components of the electroencephalogram for artifact correction. *J. Neurosci. Methods* **2015**, *250*, 47–63. [[CrossRef](#)] [[PubMed](#)]
29. Kharchenko, O.I.; Lonin, Y.F.; Zabrodina, L.P. Separation of electroencephalogram low-frequency components on the basis of the stochastic resonance effect. *Probl. At. Sci. Technol.* **2021**, *134*, 135–137. [[CrossRef](#)]
30. Sidorenko, A.V.; Voitikova, M.V. Wavelet analysis of electroencephalographic signals in microwaves. In *Biomedical Technology in Radioelectronics*; Radiotekhnika: Moscow, Russia, 2004; pp. 50–57.
31. Bassam, N.A.; Ramachanrad, V.; Parameswaram, S.E. Wavelet theory and application in communication and signal processing. In *Wavelet Theory*; Mohammady, S., Ed.; IntechOpen: London, UK, 2021; pp. 145–256.
32. Chao, B.; Chung, W.; Shih, Z. Earth’s rotation variations: A wavelet analysis. *Terra Nova* **2014**, *26*, 260–264. [[CrossRef](#)]
33. Bing, J.; Hosseini, Z.; Wang, L. Spectral Wavelet-feature Analysis and Classification Assisted Denoising for enhancing magnetic resonance spectroscopy. *NMR Biomed.* **2021**, *34*, e4497–e4511.
34. Al-Badour, F.; Sunar, M.; Cheded, L. Vibration analysis of rotating machinery using time–frequency analysis and wavelet techniques. *Mech. Syst. Signal Process.* **2011**, *25*, 2083–2101. [[CrossRef](#)]
35. Arfaou, S.; Mabrouk, A.B.; Cattani, C. *Wavelet Analysis. Basic Concepts and Applications*; Chapman and Hall, CRC: Boca Raton, FL, USA, 2021; pp. 139–254.
36. Merry, R.J.E. *Wavelet Theory and Applications, a Literature Study*; Eindhoven University of Technology, Department of Mechanical Engineering Control Systems Technology Group: Eindhoven, The Netherlands, 2005; pp. 5–41.

**Disclaimer/Publisher’s Note:** The statements, opinions and data contained in all publications are solely those of the individual author(s) and contributor(s) and not of MDPI and/or the editor(s). MDPI and/or the editor(s) disclaim responsibility for any injury to people or property resulting from any ideas, methods, instructions or products referred to in the content.